

Shaving diffusion tensor images in discriminant analysis: A study into schizophrenia

M.W.A. Caan^{a,b,*}, K.A. Vermeer^{a,c}, L.J. van Vliet^a, C.B.L.M. Majoie^b, B.D. Peters^b,
G.J. den Heeten^b, F.M. Vos^{a,b}

^a *Quantitative Imaging Group, Delft University of Technology, Lorentzweg 1, 2628 CJ, Delft, The Netherlands*

^b *Department of Radiology, Academic Medical Center, Amsterdam, The Netherlands*

^c *Rotterdam Eye Hospital, Rotterdam, The Netherlands*

Received 7 March 2005; received in revised form 13 April 2006; accepted 19 July 2006

Available online 11 September 2006

Abstract

A technique called ‘shaving’ is introduced to automatically extract the combination of relevant image regions in a comparative study. No hypothesis is needed, as in conventional pre-defined or expert selected region of interest (ROI)-analysis. In contrast to traditional voxel based analysis (VBA), correlations within the data can be modeled using principal component analysis (PCA) and linear discriminant analysis (LDA). A study into schizophrenia using diffusion tensor imaging (DTI) serves as an application. Conventional VBA found a decreased fractional anisotropy (FA) in a part of the genu of the corpus callosum and an increased FA in larger parts of white matter. The proposed method reproduced the decrease in FA in the corpus callosum and found an increase in the posterior limb of the internal capsule and uncinat fasciculus. A correlation between the decrease in the corpus callosum and the increase in the uncinat fasciculus was demonstrated.

© 2006 Elsevier B.V. All rights reserved.

Keywords: Shaving; Principal component analysis; Linear discriminant analysis; Diffusion tensor imaging; Schizophrenia

1. Introduction

Over the past few years, diffusion tensor imaging (DTI) (Basser et al., 1994a,b) has provided important insights in the structure of the brain. DTI measures the amount and direction of the diffusion of water. In white matter, the diffusion of water is anisotropic, parallel to the nerve direction, whereas in gray matter the diffusion is more isotropic. The diffusion is often characterized by a rank-2 tensor, from which scalar measures can be derived such as the fractional anisotropy (FA) and apparent diffusion coefficient (ADC).

A still growing number of studies analyze DTI to determine changes in brain structure in schizophrenia. Schizophrenia is a cognitive disorder occurring in about 1% of

the world population. The first symptoms usually occur at early adolescence, with signs of abnormal social behavior and hallucinations. Studying DTI-data of schizophrenics and controls is challenging, since there is no clear hypothesis specifying where differences are to be expected. What is generally assumed however, is that schizophrenia affects white matter structure in the brain (Shenton et al., 2001).

Typically, schizophrenia is studied by way of a region of interest (ROI)-analysis or voxel-based analysis (VBA) (Kanaan et al., 2005). In the former method, mean values of pre-defined or expert selected regions in a patient and control group are compared. The latter method consists of a comparison per individual voxel. The main findings reported are a decreased FA in the corpus callosum (Agartz et al., 2001; Ardekani et al., 2003; Foong et al., 2000; Hubl et al., 2004) and cingulum (Ardekani et al., 2003; Kubicki et al., 2003; Sun et al., 2003; Wang et al., 2003), but changes in various other white matter regions have been

* Corresponding author. Tel.: +31152783221; fax: +31152786740.

E-mail address: m.w.a.caan@tudelft.nl (M.W.A. Caan).

reported as well (Kanaan et al., 2005). Clearly, the regions in the brain are highly interacting with each other, such that a correlation between the reported regions with a decreased FA might be expected. This correlation is modeled neither by ROI-analysis nor VBA, because they consider the regions or voxels independently and thus analyze them separately. Another drawback of ROI-analysis is that expert knowledge, needed in annotating the ROIs, is subject to variation. A voxel-based analysis method is therefore preferred, although it is extremely sensitive to a misregistration of the data, a problem that gets worse with increasing resolution of modern scanners. A voxel-wise comparison of the data is then unjustified.

Despite of the mentioned drawbacks, doing ROI-analysis or VBA is still common practice in clinical studies. The analysis would be greatly strengthened by a new model that combines the advantages of both previous methods. As in VBA, no prior knowledge on correlating regions should be required. The result would be regions, containing multiple voxels related to brain regions, showing differences between the populations, comparable to a ROI-analysis. Such a model may have more discriminative power and better describe the underlying process of the disease.

In this paper, a machine learning framework will be presented that meets the previously mentioned requirements. Principal component analysis (PCA) and linear discriminant analysis (LDA) are used to mutually weight the voxels, such that correlation within the data can be modelled. A small study using PCA/LDA has been done earlier (Zhu et al., 2005). We propose a technique called ‘shaving’ (Hastie et al., 2000) to automatically extract the set of voxels separating patients from controls. By seeking a set of voxels, spatial correlation is incorporated in shaving. No expert knowledge is introduced in the whole process. A study into schizophrenia serves as an application; the proposed framework can potentially be applied to many other comparative studies.

2. Materials and methods

2.1. Subjects

Male patients admitted to the Adolescent-clinic of the Academic Medical Center in Amsterdam, The Netherlands and between 18 and 28 years of age were consecutively included. Patients had a clinical diagnosis of recent-onset schizophrenia or a related disorder according to DSM-IV criteria (American Psychiatric Association, 1994). All patients received antipsychotic medication.

Exclusion criteria were: history of a demonstrable neurological or endocrine disease, history of a head trauma with loss of consciousness for more than 15 min, mental retardation, gross brain abnormalities on conventional MRI and substance abuse within one week of MRI-acquisition. Additional exclusion criteria for controls were: lifetime diagnosis of substance abuse and a personal or family history of a major psychiatric illness such as schizophrenia. Controls

were matched to patients for gender, age, educational level and handedness. This study was approved by the local medical and ethical committee. After complete description of the study to the subjects, written consent was obtained.

After the clinical condition of the patients had stabilized, patients were interviewed by a research staff member who was not involved in the treatment. Date of the first psychotic episode and educational level were assessed. The start of the first psychotic episode was defined as the moment when patients experienced hallucinations, delusions or disorganized behavior/speech during most part of the day, during at least one week. Handedness was determined using the Annett handedness questionnaire (Annett, 1970).

2.2. Data acquisition

MR diffusion tensor imaging was performed on a 1.5T Siemens Visions (VB33E, Siemens, Erlangen, Germany). A spin-echo EPI sequence with an extra 180° pulse and balanced diffusion sensitizing gradients was used to minimize artifacts induced by eddy currents (Reese et al., 2003). Other imaging parameters were: diffusion weighting $b = 1000 \text{ s/mm}^2$, voxel-size $2 \times 2 \times 6.5 \text{ mm}$, TE (echo time) 109 ms, six icosahedric diffusion directions (Akkerman, 2003).

2.3. Data preprocessing

The diffusion is described by a 3×3 symmetric tensor \mathbf{D} , from which eigenvectors e_i and eigenvalues λ_i can be calculated. The diffusion tensor can be visualized by an ellipsoid. The eigenvectors are the axes of the ellipsoid, the eigenvalues determine the shape and size of the ellipsoid. The fractional anisotropy (FA) (Basser and Pierpaoli, 1996) is a scalar measure derived from the tensor and written as

$$\text{FA} = \frac{\sqrt{(\lambda_1 - \lambda_2)^2 + (\lambda_2 - \lambda_3)^2 + (\lambda_3 - \lambda_1)^2}}{\sqrt{2} \sqrt{\lambda_1^2 + \lambda_2^2 + \lambda_3^2}}, \quad (1)$$

which ranges from 0 (isotropic) to 1 (anisotropic). Tensor representations for some FA-values are displayed in Fig. 1. The FA is commonly used in brain studies in which changes in brain structure are expected (Kanaan et al., 2005). This is based on the assumption that a reduction of FA in white matter corresponds to a reduction in white matter integrity.

The diffusion weighted images (DWIs) were isotropically resampled to $2 \times 2 \times 2 \text{ mm}$, allowing sub-voxel translations in the z -plane in registration. Moreover, the DWIs were smoothed with a Gaussian kernel of 2 mm, thereby reducing the occurrence of high FA due to noise and limiting the negative side-effects of possible misregistration. When isotropically smoothing DWIs, there is a risk of mixing up intensities related to bundles with different orientations. However, considering the relatively low spatial resolution of the acquisitions, this effect will be negligible.

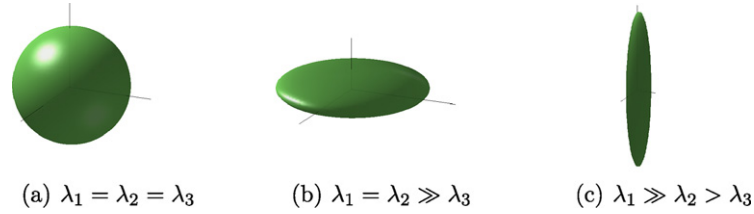


Fig. 1. Three tensor representations with FA-values 0 , $\sim \frac{1}{\sqrt{2}}$ and ~ 1 , respectively.

In a voxel-based analysis, a proper registration is not only essential but also a challenging task, due to large variability in inter-subject anatomy. Solely an affine transformation will not map the volumes onto the same frame of reference. Therefore, a non-rigid registration using the demons algorithm (Thirion, 1998) was added to an affine transformation using 12 degrees of freedom. The registration was done directly on the FA-images in 3D-Slicer, using the FA computed from an DTI-atlas (Wakana et al., 2004) as target. In order to avoid local minima in the non-rigid registration, an image pyramid was built with subsampled copies of the data. Registration was performed at each level, starting at the top and moving one level down after convergence of the demons algorithm. The deformation field, a 3D-vector field, was regularized by smoothing using a Gaussian kernel with $\sigma = 1$.

After registration, a threshold of 0.25 was applied to the FA, restricting the analysis to white matter (Alexander et al., 2000), which is expected to be affected by schizophrenia (Shenton et al., 2001).

2.4. Algorithm design

A new algorithm will now be described, aiming to automatically detect regions that discriminate patients from controls. This is done by ‘shaving’ the voxel space, based on the mapping computed by PCA/LDA. Classification is done during shaving to validate if the populations can still be discriminated based on the information stored in the preserved regions.

2.4.1. Mapping computation

Let us now briefly review PCA/LDA-analysis. The patient and control group are denoted ω_p and ω_c , the so-called classes. Let m_p and m_c be the number of patients and controls, summing to m , the size of the cohort. The n voxels to be studied are reshaped to n -dimensional vectors x_i ($i = 1, \dots, m$), where the ordering is chosen arbitrarily.

Thus, each image can be regarded as a point in an n -dimensional space \mathbb{R}^n . In general, the cohort size is much smaller than the number of voxels ($m \ll n$), making the problem of discriminating data in this space highly ill-posed. This is called the *small sample size problem* (Fukunaga, 1990), for which a unique solution does not exist. PCA/LDA solves this problem in a two-step way of dimensionality reduction, $\mathbb{R}^n \xrightarrow{\text{PCA}} \mathbb{R}^r \xrightarrow{\text{LDA}} \mathbb{R}$ (Huang et al., 2002), such that a one-dimensional x_i^* is obtained:

$$x_i^* = a^T(x_i - \bar{x}), \quad (2)$$

where \bar{x} is the mean over all x_i and a is written as

$$a = Pq. \quad (3)$$

The matrix $P_{n \times r}$ maps a point from \mathbb{R}^n to \mathbb{R}^r . It contains only non-singular eigenvectors or principal components of the total scatter matrix $S_t = \sum (x_i - \bar{x})(x_i - \bar{x})^T$ (Turk and Pentland, 1991). The order of eigenvectors is such that the corresponding eigenvalues are monotonically increasing. If $r = m - 1$, all variance in the data is retained; lowering r yields a loss of information. A proper choice of r will be discussed later on. Projecting x_i onto P results in vectors $x_i' = P^T(x_i - \bar{x})$ of length r .

The vector q of size r is found by LDA, aiming to discriminate patients from controls in a one-dimensional space \mathbb{R} . q is computed in the low-dimensional subspace \mathbb{R}^r and written as (Duda and Hart, 2001)

$$q = S_w^{-1} S_b, \quad (4)$$

with the class-within scatter matrix $S_w = \frac{1}{m} \sum_{j=1}^2 \sum_{i=1}^{m_j} (x_i' - \bar{x}_j')(x_i' - \bar{x}_j')^T$ and the class-between scatter matrix $S_b = \frac{1}{m} \sum_{j=1}^2 (\bar{x}_j' - \bar{x}')(\bar{x}_j' - \bar{x}')^T$ for the two-class case and the mean of class j notated as \bar{x}_j' .

2.4.2. Classification

Now the data can be projected onto x^* using Eq. (2). In the remainder of this paper, it is assumed that $\bar{x}_{\omega_p}^* < \bar{x}_{\omega_c}^*$ (x^* is mirrored if this is not the case). Classification with a simple classifier, the nearest-mean classifier, is done on x^* . The classification error is computed by means of cross-validation (Duda and Hart, 2001).

Fivefold cross-validation randomly divides the data into five groups of approximately equal size and with the same proportion of the classes. Now four groups are used as training set, for computing a , and one group is used as testing set, which is mapped onto a for computing the classification error. This is done five times, each time rotating the data in the training and testing sets, resulting in five errors computed on the individual groups, which are averaged. The cross-validation is repeated 10 times, with different composition of the cross-validation groups, after which a mean error is computed. The 95%-confidence region of the error depends on the error and size of the cohort (Duda and Hart, 2001). If the upper boundary is below 50%, a significant difference between patients and controls is concluded. An estimate of the stability of the classification error is given by the standard deviation of the error over

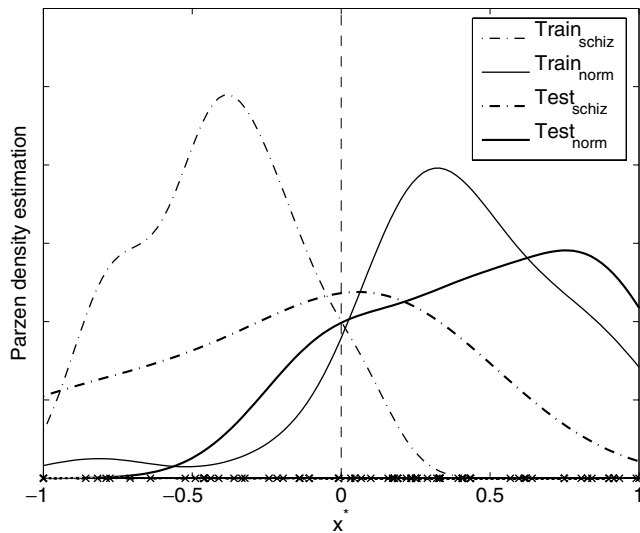


Fig. 2. x^* with Parzen density estimation plotted for a training and testing set. The vertical dashed line indicates the decision boundary.

the 10 repeated cross-validations. As an illustration, x^* is plotted for one training and testing set in the cross-validation, with a corresponding Parzen density estimation, in Fig. 2.

Cross-validation is used to choose r , the dimensionality of the subspace where LDA is performed. The first principal components are expected to describe most variance in the data, whereas the last only describe noise. The error is therefore expected to lower until a certain minimum, which defines the value of r . The classification error is computed ‘forward’, starting with the first and using an increasing number of principal components. A second experiment, in which the classification error is computed ‘backward’, verifies if the last components indeed describe noise. Starting with the trailing principal component, more and more leading principal components are added until at the end all are used. The error should in this case remain close to 50% until the leading principal components are added.

2.4.3. Visualization

It is clinically important to know which regions of the brain manifest a significant difference between the populations (as indicated by the FA). The mapping a computed by the PCA/LDA-algorithm will therefore be analyzed to identify those regions. a describes how the voxels are mutually weighted for discriminating patients from controls; in other words, it reflects how voxels are combined to separate the populations. The regions where $|a|$ is high contribute most to the separation in x^* (notice that $\bar{x}^* = 0$ due to the subtraction of the mean from the data).

Differences between patients and controls are expected to emerge in regions related to known anatomical brain regions. ‘Shaving’ is proposed as a way to automatically extract the set of voxels separating patients from controls. By seeking a set of discriminating voxels, spatial correlation is incorporated in shaving. This technique was origi-

nally applied to genes, to identify subsets of genes with similar expression patterns (Hastie et al., 2000). It iteratively removes voxels with small $|a|$ and then re-trains the remaining voxels, such that the mutual weighting of the voxels is adapted. A constraint is added to this procedure to remove in each iteration small objects from a .

The shaving procedure is as follows:

- (1) Consider all n voxels, $V = \{1, 2, \dots, n\}$.
- (2) Compute a for all voxels in V in m images $\{x_i(j) | i = 1 \dots m, j \in V\}$.
- (3) Let $P = \{j | a(j) > 0\}$ and $N = \{j | a(j) \leq 0\}$.
- (4) Remove objects smaller than s_{\min} voxels from P and N .
- (5) Let $V = P \cup N$.
- (6) Discard 25% of the voxels with the smallest value of $|a(V)|$ from set V .
- (7) Repeat from step 2 until the desired percentage of voxels is left.

The stopping criterion is determined by studying the classification error as a function of the fraction of retained voxels. The error is expected to initially decrease due to removal of noise, after which it increases when the discriminating regions are being shaved off. The expected minimum of this error curve is used to determine at which fraction of voxels shaving is terminated. Note that the number of principal components r is determined in a separate cross-validation, before shaving. As a result of the shaving process, the combination of regions discriminating the two populations is automatically extracted from the data.

2.5. Algorithm evaluation

The behavior of the proposed shaving algorithm is studied by means of simulated data, containing regions whose mean values are correlated. It will be investigated if r can properly be chosen, how the classification error behaves during shaving and if the resulting discriminating regions match with the generated ones. For comparison, VBA of this data will be done.

In order to study the reliability of the algorithm, two tests are performed, regarding overtraining and stability. In the first test, patients and controls are randomly divided into two classes, containing the same proportion of the initial populations. If the classification error on this data is significantly lower than 50%, the used classifier is over-trained. In the second test the stability of the algorithm is evaluated. The regions the algorithm comes up with should not change much while adding or removing a subject to or from the cohort. The stability is tested by a jack-knife procedure (Duda and Hart, 2001). Given m images, the classifier is trained m times, each time removing one of the images from the full set. For each object in a that is found, the number of occurrences in each result is computed. Objects showing up in more than 90% of the steps are considered to be stable and are displayed as a final result.

The hypothesis of correlation in the data is verified by doing LDA on the mean values of the regions resulting from the shaving algorithm. The extent to which the regions are mutually weighted gives an indication of the existence of correlation.

3. Results

3.1. Simulated data

The behavior of the shaving algorithm was studied using simulated data. Two classes containing 36 and 24 images of size 100×100 were generated, containing a circle and a ring both of constant intensity. The intensities of the two objects were chosen such that they are correlated, see Fig. 3. Zero-mean Gaussian white noise with $\sigma = 10$ was added to the data, such that the SNR was approximately equal to the SNR of DTI (Hunsche et al., 2001). The data were smoothed using a Gaussian kernel with $\sigma = 1$.

A parameter sweep was performed for choosing the optimal number of principal components r . The classification error after cross-validation is plotted in Fig. 4, using up to 45 principal components computed on the training set. Both in the ‘forward’- and ‘backward’-experiment, the error drops to zero when the second principal component is added. This component is perpendicular to the direction of most variation; it can be concluded from Fig. 3(a) that best discrimination is achieved in this direction.

Fig. 5(a) shows the results of the shaving procedure. In the top image, the remaining voxels during shaving are shown, the bottom image displays the corresponding mapping a . The result of a VBA using statistical parametric mapping (SPM) (Friston et al., 1995) with $P < 0.001$ and a minimal object size of 10 voxels is given in Fig. 5(b). What catches the eye, is that VBA only found the mean difference in the circle and not in the ring,

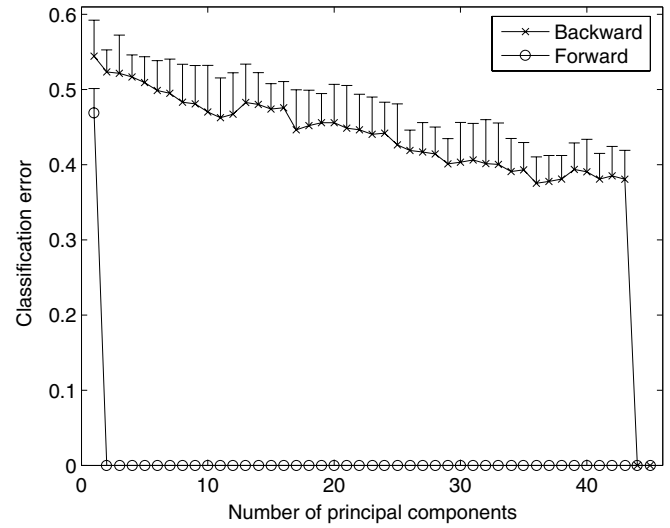


Fig. 4. Classification error using the simulated data as a function of the number of principal components used, with error bars denoting the standard deviation of the error. See the text for an explanation of the ‘forward’- and ‘backward’-experiment.

because the data was generated with different class means in the former and equal class means in the latter feature. Because the proposed algorithm was able to model correlation in the data, it resulted in a combination of the ring and the circle.

The classification error cannot be used as stopping criterion in this experiment, because the classes were perfectly separable using the subsequent mappings presented in Fig. 5(a). Based on visual inspection, 10% is an optimal fraction of voxels to use, because then background noise has been removed whereas the generated structures remain intact. This example demonstrates the potential power of shaving; its performance on real data will now be discussed.

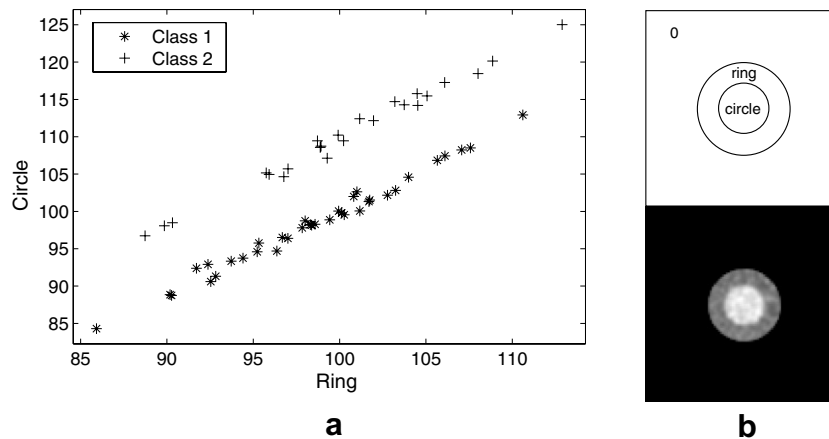


Fig. 3. (a) Scatterplot of the mean intensity values in the simulated data, generated with class means $(100 \ 100)$ and $(100 \ 110)$, and equal covariance matrix $\begin{pmatrix} 40 & 35 \\ 35 & 40 \end{pmatrix}$. (b) The design used to generate the simulated data (top) and an example image of class 2, at intensity interval $(95 \ 125)$ to enhance contrast (bottom).

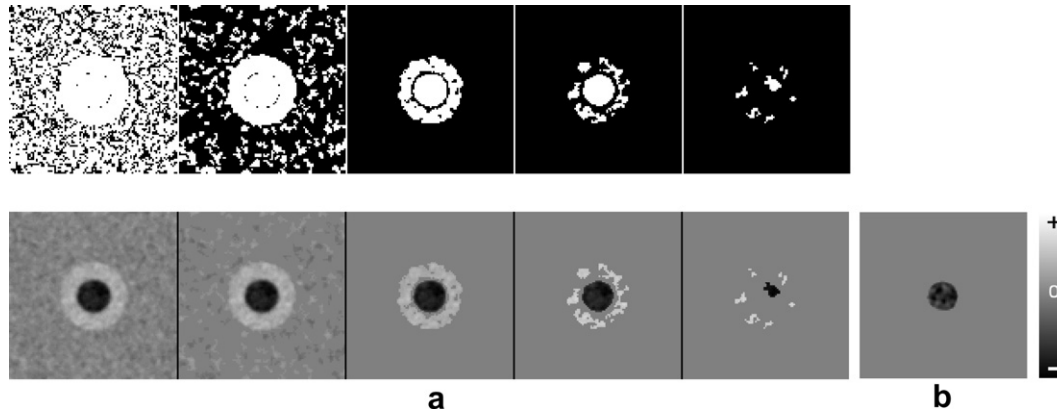


Fig. 5. (a) Illustration of the 'shaving'-procedure: the remaining voxels in white (top) and the corresponding mapping a (bottom) of the simulated data after shaving to 75%, 32%, 10%, 6% and 1.3%, respectively. (b) Two-sided conventional VBA ($P < 0.001$) of the simulated data.

3.2. Experimental data

Thirty-four male patients were included with an average age of 22.3 years and a standard deviation of 2.6 years. They were compared with 24 healthy controls with an average age of 22.5 years and a SD of 3.2 years. Handedness of patients was (right/left/ambidexter) 85/12/3%, of controls it was 87/13/0%. Educational level of patients was: 29% skilled training, 32% bachelor level and 38% master level; of controls 29%, 29% and 42%, respectively. No gross abnormalities could be detected on conventional MR imaging by an expert. Eddy current induced morphing in the phase direction was visually esteemed to be negligible.

In order to apply PCA/LDA and shaving, a threshold value s_{\min} had to be chosen for objects to be removed in the shaving process, as described in Section 2.4. s_{\min} was set to 50 voxels (1.6 cm^3), which is a typical size of brain

tracts where changes are expected (Hermann et al., 2003). The number of principal components r was chosen based on the classification error after cross-validation, as can be seen in Fig. 6. The 'forward'-experiment makes clear that $r = 13$ is the optimal number of components, since adding more components does not lower the error and increases the standard deviation in the error. The 'backward'-experiment, starting with the last and adding leading components, reveals that the trailing principal components are indeed describing noise, because the error is close to 50%. As in the simulated data experiment, the standard deviation in the error decreases when leading principal components are included.

The classification error as a function of the fraction of voxels retained after shaving is shown in Fig. 7. This figure reveals only a slight increase in the error during shaving; shaving is chosen to be terminated at 0.3%. The minimal classification error of 25%, with the upper boundary of

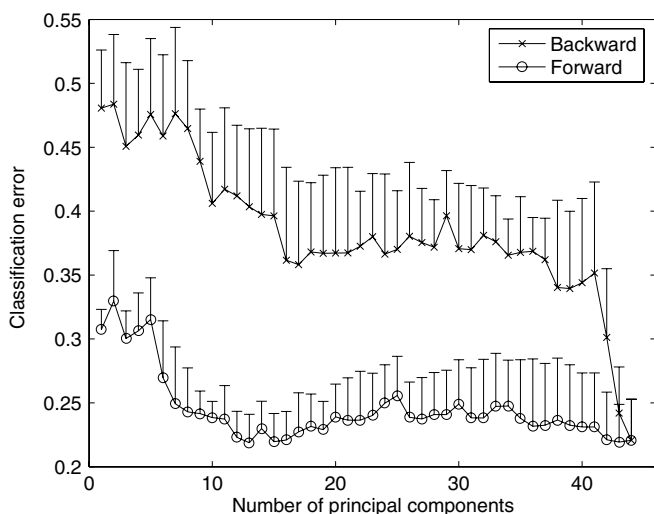


Fig. 6. Classification error using the FA as a function of the number of principal components used, with error bars denoting the standard deviation of the error. See the text for an explanation of the 'forward'- and 'backward'-experiment.

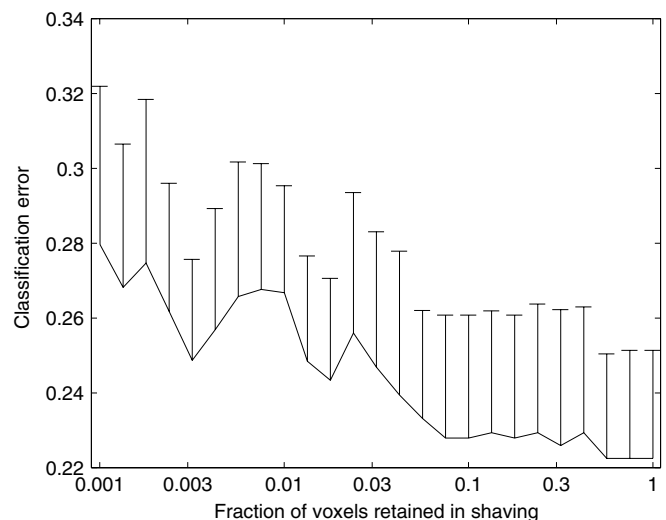


Fig. 7. Classification error using the FA as a function of the fraction of voxels retained in shaving, with error bars denoting the SD of the error. The 'forward'- and 'backward'-experiment start with the first and last principal component, respectively and end using all components.

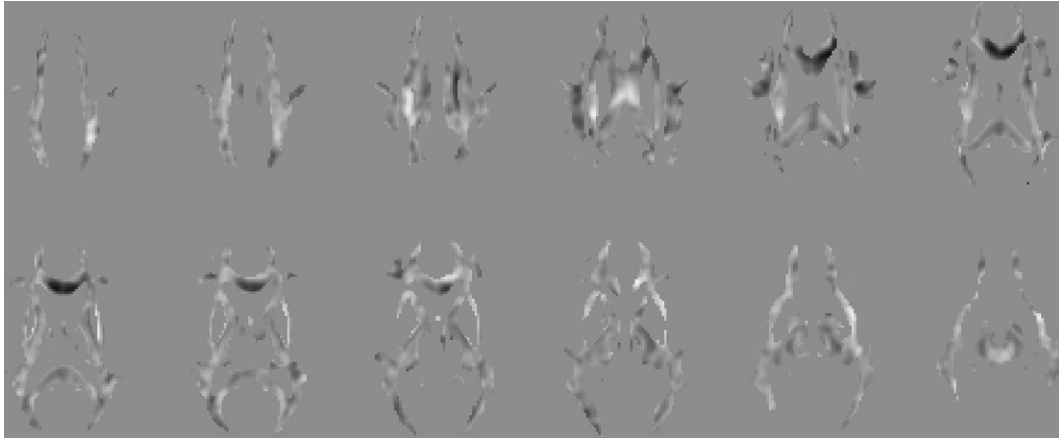


Fig. 8. The mapping a computed using PCA/LDA of FA-images before shaving. a is zero on the gray background, negative in black and positive in white regions.

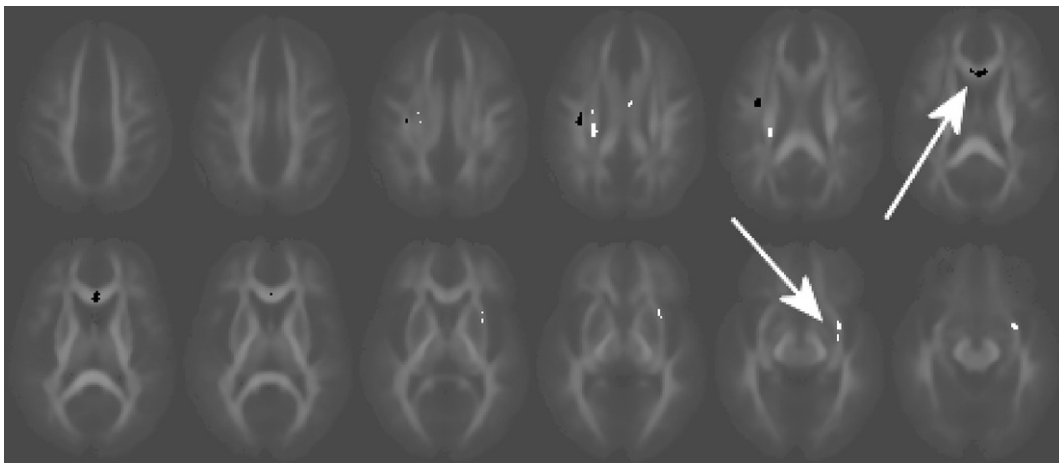


Fig. 9. Only the stable regions in a after shaving to 0.3% of the total number of voxels. White regions indicate an increased FA, black regions a decreased FA. The average FA is shown in gray on the background. The arrows point to the decrease in the corpus callosum and the increase in the uncinate fasciculus.

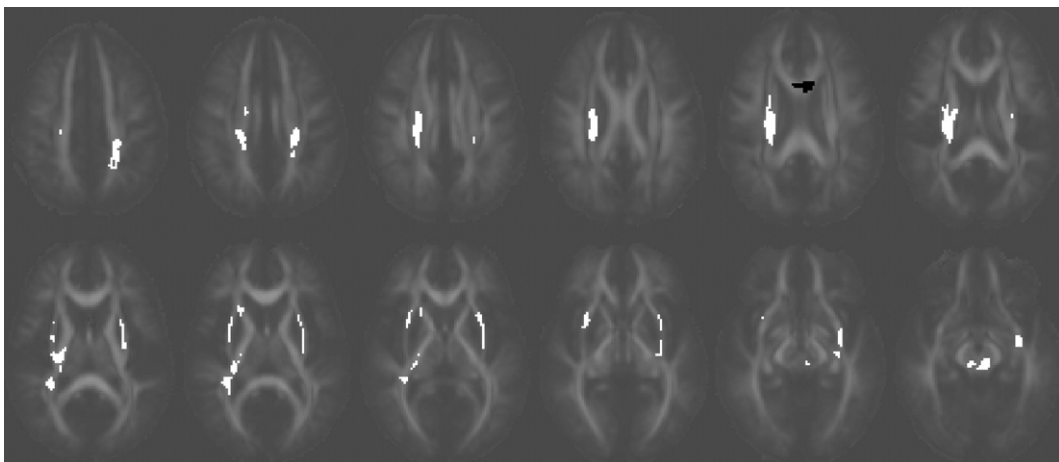


Fig. 10. Two-sided VBA ($P < 0.001$) of the FA. White regions indicate an increased FA, black regions a decreased FA. The average FA is shown in gray on the background.

the 95%-confidence interval at 35% (Duda and Hart, 2001), means a significant difference between patients and controls.

The PCA/LDA mapping a before shaving is shown in Fig. 8. The mapping after shaving to 0.3% and with unstable regions discarded can be seen in Fig. 9. These results are interpreted as a decrease in the genu of the corpus callosum and an increase in the right uncinate fasciculus and posterior limb of the internal capsule.

VBA using SPM (Friston et al., 1995) was applied, keeping voxels with $P < 0.001$ and a minimal object size of 20 voxels. The result is displayed in Fig. 10. A significantly lower FA can be seen in the genu of the corpus callosum, which disappears when increasing the object size threshold to 50 voxels as used in shaving. A higher FA is observed in the posterior limb of the internal capsule, as well as in several inferior white matter regions.

After that the results were calculated, the algorithm was tested on overtraining. The classification error of randomly composed classes before shaving yielded 62%, lowering to 42% when 0.1% of the voxels are used. The upper boundary of the 95%-confidence regions then equals 55%, such that a significant difference between these classes cannot be concluded.

Finally, LDA was performed on the mean values of two resulting regions of the shaving procedure, situated in the corpus callosum and uncinate fasciculus. These mean values are scatter plotted in Fig. 11, with the classification boundary computed by LDA. The slope of this boundary indicates that the classifier equally weights the regions, indicating a correlation between them. The classification error after cross-validation equals 25%, comparable to the error after shaving.

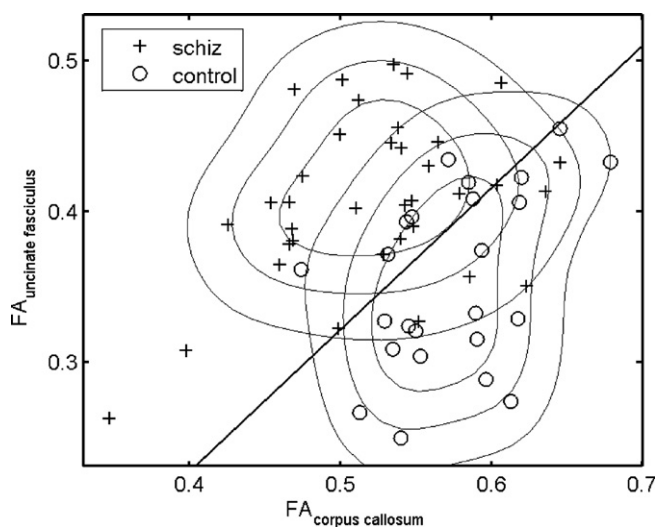


Fig. 11. Scatter plot of the mean FA-values of the regions in the corpus callosum and uncinate fasciculus found with shaving, with the classification boundary given by LDA.

4. Discussion and conclusion

We introduced a new machine learning framework for comparative studies on volumetric data. By ‘shaving’ the mapping computed by PCA/LDA, a combination of characteristic regions is automatically extracted. In this way, a solution is found to a shortcoming of both ROI-analysis and VBA, namely that they do not take correlation between regions into account.

The method was applied to DTI-data of schizophrenics and controls, which resulted in a classification error of 25% after shaving to 0.3% of the voxels. The discriminating regions correlated with a decrease in FA in the genu of the corpus callosum and an increase in the right uncinate fasciculus and posterior limb of the internal capsule. Conventional VBA found a decrease in FA in the corpus callosum and an increased FA in various white matter regions, including those found using the proposed algorithm, which is unprecedented (Kanaan et al., 2005). The shaving algorithm localizes the differences more accurately, such that they can be better interpreted. The correlation in the data was demonstrated by LDA of the means of the regions of the corpus callosum and the uncinate fasciculus (see Fig. 11).

The number of principal components is a critical parameter, affecting the behavior of the algorithm. Including too few components will only allow for describing global differences, whereas including too many might result in fitting the model to the noise. Based on a parameter sweep embedded in cross-validation, 13 principal components were used. With only 60 subjects available, LDA was computed in a sparsely sampled space, which can make the algorithm unstable and thus unreliable. The stability was ensured by only keeping the regions showing up in more than 90% of the steps in a jack-knife procedure. The reliability was demonstrated by an insignificant classification error of 42% on two randomly composed classes.

It was not our intention to use the classifier in clinical practice, judging whether a new subject is schizophrenic or not, although it is theoretically possible. Rather, we use the method only to identify significant differences between patients and controls.

PCA is driven by the total variance, such that non-brain regions largely influence the classifier, as they cover approximately 50% of the voxels. The experiment with simulated data has shown that shaving is able to remove these regions before eliminating characteristic regions. Still, a threshold was applied to the experimental data for two reasons. First, only differences in white matter were a priori expected (Shenton et al., 2001). Second, only the main white matter tracts were observed to be aligned after registration, such that voxel-wise analysis of other brain regions was not allowed.

Not having any knowledge about the type of correlation present in the data, a linear correlation was modeled in the algorithm. A possible extension is using a non-linear (kernel-based) classifier instead of PCA/LDA. This may

lead to a lower classification error, if the correlation is indeed better modeled non-linearly. However, there is no standard solution for the problem of how to localize and visualize differences using such a classifier.

The observed decrease in the corpus callosum was found several times before (Agartz et al., 2001; Ardekani et al., 2003; Foong et al., 2000; Hubl et al., 2004), whereas a finding of higher FA is almost unprecedented. The increase in the posterior limb of the internal capsule may be explained by the fact that in this region tracts are crossing (Wiegell et al., 2000). Then the second-order diffusion tensor model does not hold and care must be taken in interpreting changes in FA.

In this paper, the focus was on the methodology of the shaving algorithm. Future work will be on gathering and studying higher-resolitional data, in order to validate the findings. Incorporating correlation in analysis is a new step in pathological studies, opening the way to more knowledge of brain diseases in the future.

Acknowledgement

The authors thank Dr. R.P.W. Duin for his support. The involvement of M.W.A. Caan in this work took place in the context of the Virtual Laboratory for e-Science project (<http://www.vl-e.nl/>). This project is supported by a BSIK grant from the Dutch Ministry of Education, Culture and Science (OC&W) and is part of the ICT innovation program of the Ministry of Economic Affairs (EZ).

References

- Agartz, I., Andersson, J., Skare, S., 2001. Abnormal brain white matter in schizophrenia: a diffusion tensor imaging study. *Neuroreport* 12, 2251–2254.
- Akkerman, E., 2003. Efficient measurement and calculation of MR diffusion anisotropy images using the platonic variance method. *Magn. Reson. Med.* 49, 599–604.
- Alexander, A., Hasan, K., et al., 2000. A geometric analysis of diffusion tensor measurements of the human brain. *Magn. Reson. Med.* 44, 283–291.
- American Psychiatric Association (APA), 1994. *DSM-IV: Diagnostic and Statistic Manual of Mental Disorders*, fourth ed. APA, Washington, DC.
- Annett, M., 1970. A classification of hand preference by association analysis. *Br. J. Psychol.* 61 (3), 303–321.
- Ardekani, B., Nierenberg, J., et al., 2003. MRI study of white matter diffusion anisotropy in schizophrenia. *Neuroreport* 14, 2025–2029.
- Basser, P., Pierpaoli, C., 1996. Microstructural and physiological features of tissues elucidated by quantitative-diffusion-tensor MRI. *J. Magn. Reson. B* 111, 209–219.
- Basser, P., Mattiello, J., Bihan, D.L., 1994a. Estimation of the effective self-diffusion tensor from the NMR spin echo. *J. Magn. Reson. B* (103), 247–254.
- Basser, P., Mattiello, J., Bihan, D.L., 1994b. MR diffusion tensor spectroscopy and imaging. *Biophys. J.* 66, 259–267.
- 3D-Slicer, Tool for visualization, registration and segmentation. Available from: <<http://www.slicer.org>>.
- Duda, R., Hart, P., 2001. *Pattern Classification*. Wiley, New York.
- Foong, J., Maier, M., et al., 2000. Neuropathological abnormalities of the corpus callosum in schizophrenia: a diffusion tensor imaging study. *J. Neurol. Neurosurg. Psychiatry* 68, 242–244.
- Friston, K., Holmes, A., et al., 1995. Statistical parametric maps in functional imaging: a general linear approach. *Hum. Brain Mapp.* 2, 189.
- Fukunaga, K., 1990. *Introduction to Statistical Pattern Recognition*. Academic Press, New York.
- Hastie, T., Tibshirani, R., et al., 2000. Gene shaving as a method for identifying distinct sets of genes with similar expression patterns. *Genome Biol.* 1 (2), research0003.1–0003.21.
- Hermann, B., Hansen, R., et al., 2003. Neurodevelopmental vulnerability of the corpus callosum to childhood onset localization-related epilepsy. *Neuroimage* 18, 284–292.
- Huang, R., Liu, Q., et al., 2002. Solving the small sample size problem of LDA. *Proc. Int. Conf. Pattern Recognition* 3, 29–32.
- Hubl, D., Koenig, T., et al., 2004. Pathways that make voices. *Arch. Gen. Psychiatry* 61, 658–668.
- Hunsche, S., Mosely, M., et al., 2001. Diffusion-tensor MR imaging at 1.5 and 3.0 T: Initial observations. *Radiology* 221, 550–556.
- Kanaan, R., Kim, J., et al., 2005. Diffusion tensor imaging in schizophrenia. *Biol. Psychiatry* 58 (12), 921–929.
- Kubicki, M., Westin, C., et al., 2003. Cingulate fasciculus integrity disruption in schizophrenia: a magnetic resonance diffusion tensor imaging study. *Biol. Psychiatry* 54, 1171–1180.
- Reese, T., Heid, O., et al., 2003. Reduction of eddy-current-induced distortion in diffusion MRI using twice-refocused spin echo. *Magn. Reson. Med.* 49, 177–182.
- Shenton, M., Dickey, M., et al., 2001. A review of MRI findings in schizophrenia. *Schizophr. Res.* 49, 1–52.
- Sun, Z., Wang, F., et al., 2003. Abnormal anterior cingulum in patients with schizophrenia: a diffusion tensor imaging study. *Neuroreport* 14, 1833–1836.
- Thirion, J.-P., 1998. Image matching as a diffusion process: an analogy with Maxwell's demons. *Med. Image Anal.* 2 (3), 243–260.
- Turk, M., Pentland, A., 1991. Eigenfaces for recognition. *J. Cognitive Neurosci.* 3, 71–86.
- Wakana, S., Jiang, H., et al., 2004. Fiber tract-based atlas of human white matter anatomy. *Radiology* 230, 77–87.
- Wang, F., Sun, Z., et al., 2003. Anterior cingulum abnormalities in male patients with schizophrenia determined through diffusion tensor imaging. *Am. J. Psychiatry* 161, 573–575.
- Wiegell, M., Larsson, H., et al., 2000. Fiber crossing in human brain depicted with diffusion tensor MR imaging. *Radiology* 217, 897–903.
- Zhu, C., Zang, Y., et al., 2005. Discriminative analysis of brain function at resting-state for attention-deficit/hyperactivity disorder. In: *Proceedings of the MICCAI'05, LNCS*, vol. 3750, pp. 468–475.